

Marquette University

e-Publications@Marquette

Master's Theses (2009 -)

Dissertations, Theses, and Professional
Projects

The Influence of Peri-Cervical Dentin Conservation on the Propagation of Cracks in Mandibular Molars

Hassanain Zaheer
Marquette University

Follow this and additional works at: https://epublications.marquette.edu/theses_open



Part of the [Dentistry Commons](#)

Recommended Citation

Zaheer, Hassanain, "The Influence of Peri-Cervical Dentin Conservation on the Propagation of Cracks in Mandibular Molars" (2023). *Master's Theses (2009 -)*. 755.
https://epublications.marquette.edu/theses_open/755

THE INFLUENCE OF PERI-CERVICAL DENTIN CONSERVATION ON
THE PROPAGATION OF CRACKS IN MANDIBULAR MOLARS

by

Hassanain Zaheer DDS

A Dissertation submitted to the Faculty of the Graduate School,
Marquette University,
in Partial Fulfillment of the Requirements for
the Degree of Master of Science

Milwaukee, Wisconsin

May 2023

ABSTRACT
THE INFLUENCE OF PERI-CERVICAL DENTIN CONSERVATION ON
THE PROPAGATION OF CRACKS IN MANDIBULAR MOLARS

Hassanain Zaheer DDS

Marquette University, 2023

Introduction: The objective of this study was to investigate the effect of peri-cervical dentin conservation during root canal treatment on the longitudinal propagation of cracks, utilizing the finite element method.

Methods: Two 3D printed mandibular molars were subjected to a simulated root canal therapy protocol. The teeth were divided into two test groups: Group 1: Instrumented with using Protaper Gold (PTG) rotary files. Group 2: Instrumented with using TruNatomy. Each access was restored with composite at the level of the CEJ to the occlusal surface. The two teeth were digitized using a high-resolution micro-computed tomographic scan to create 3-D models and stereolithographic reconstructions for Finite Element Analysis. A crack was simulated originating at the distal marginal ridge extending horizontally to the distal occlusal cavosurface, and apically 2mm above the CEJ. Each model was subjected to a 247-newton load to mimic the stress experienced during mastication.

Results: In both groups, the crack started propagating at approximately 40,000 mastication cycles. Group 1 which was instrumented with Protaper Gold, had 0.5mm of crack propagation at 60,218,000 mastication cycles. Group 2 which was instrumented with TruNatomy, had 0.5mm of crack propagation at 10,042,000 cycles.

Conclusions: Within the limitations of this study, it can be concluded that cracks propagated to a lesser extent in mandibular molars instrumented with PTG compared to TruNatomy. The propagation of the simulated crack for both PTG and TruNatomy initiated around 40,000 mastication cycles.

ACKNOWLEDGEMENTS

Hassanain Zaheer DDS

In the name of Allah, the most gracious, the most merciful.

First, I would like to thank my parents for all the sacrifices they made for me to reach this point in my career. I would like to thank my siblings for the guidance, support and paving the road for me to follow. I would not be in this position with the continuous love and support my family has provided me.

I would like to thank my co-residents for their friendship and support throughout residency. I would like to thank the Marquette Endodontics faculty for their guidance and mentorship. I am thankful to be a part of the Marquette Endo family.

TABLE OF CONTENTS

ACKNOWLEDGEMENT.....	i
LIST OF TABLES.....	iii
LIST OF FIGURES.....	iv
INTRODUCTION.....	1
LITERATURE REVIEW.....	3
MATERIALS AND METHODS.....	7
RESULTS.....	22
DISCUSSION.....	27
CONCLUSIONS.....	30
BIBLIOGRAPHY.....	31

LIST OF TABLES

Table 1: <i>Structural Properties of Enamel</i>	9
Table 2: <i>Structural Properties of Cancellous Bone</i>	10
Table 3: <i>Structural Properties of Composite</i>	10
Table 4: <i>Structural Properties of Cortical Bone</i>	10
Table 5: <i>Structural Properties of the Periodontal Ligament</i>	11
Table 6: <i>Structural Properties of Dentin</i>	11

LIST OF FIGURES

Figure 1: <i>Stereolithographic reconstruction of the scanned mandibular molar</i>	12-14
Figure 2: <i>Mastication Load distribution on occlusal surface</i>	15-16
Figure 3: <i>3D CAD models of the molar</i>	17-18
Figure 4: <i>Polygon decimation, smoothening, and refinement</i>	19-20
Figure 5: <i>Initial crack simulation and position</i>	21
Figure 6: <i>Group 1 crack propagation in mm over number of mastication cycles</i>	23
Figure 7: <i>Group 2 crack propagation in mm over number of mastication cycles</i>	24
Figure 8: <i>3D visualization of group 1 Crack propagation</i>	25
Figure 9: <i>3D visualization of group 2 Crack propagation</i>	26

INTRODUCTION

Dental providers have reported an increased number of patients with cracked teeth since the COVID-19 pandemic began. In fact, a recent study reported that the rate of cracked teeth increased during the initial outbreak of the COVID-19 pandemic and one year later (1). A 2013 study estimated a widespread prevalence of cracked teeth even before the pandemic and concluded that a “cracked tooth epidemic” exists (2). Although teeth can withstand forces that are 700N or greater (3), it is not uncommon for cracks to form, resulting in fractured teeth. One study estimated that 66.1% of patients had at least one cracked molar (2).

As the dentition ages, so does the likelihood of the formation of cracks within the teeth (2). Iatrogenic factors can also amplify the propagation of cracks during endodontic procedures due to the size/taper of root canal preparation, coronal flaring, obturation techniques, and retreatment procedures (4). Coronal flaring has been traditionally carried out by gates glidden burs, peeso eamers, or progressively tapered file systems. However, coronal flaring can result in the loss of a critical structural component known as peri-cervical dentin (PCD). The peri-cervical dentin is roughly 4 mm apical and coronal to the crestal bone. Conservation of PCD has led to a shift in preparation style of the endodontic access cavity and the design and taper of the endodontic rotary files. The shift has led to what is known as minimally invasive endodontics (MIE).

There are numerous endodontic file systems on the market that differ in cross section, metallurgy, and taper. For instance, the variable taper of the ProTaper Gold

(PTG) System (Dentsply Tulsa Dental Specialties, Tulsa, OK) has a maximum flute diameter (MFD) of 1.2 mm. In contrast, file systems with significantly smaller MFDs have been introduced to the market in an effort to conserve dentin. One such system is the TruNatomy (TRN, Dentsply Sirona) which has a MFD of 0.8mm and shapes root canal systems to a regressively tapered preparation. The null hypothesis was that crack propagation in mandibular molars is not affected by remaining PCD after root canal instrumentation with different tapered rotary files.

Multiple studies have utilized Finite Elemental Analysis (FEA) to evaluate the stress concentrations with different instrumentation protocols (3,5,6). A study by Smoljan et al. concluded that preservation of PCD may increase the fracture resistance of a tooth (7), while another FEA study concluded that coronal canal flaring has minimal effect on tooth integrity. Although the list of studies evaluating stress concentrations is extensive, there is limited research evaluating the longitudinal propagation of cracks. The Extended Finite Element Method (XFEM) has been applied to study the composite resin core level and periodontal pocket depth effects on stress distribution, and crack propagation in endodontically treated teeth (8). The aim of this study was to investigate the effect of PCD conservation during root canal treatment on the longitudinal propagation of cracks, utilizing the extended finite element method.

LITERATURE REVIEW

Crack formation

A cracked tooth is a tooth in which there exists a partial or complete fracture of a plane that experiences stress regularly (9). A stress plane results from forces during the masticatory cycle, which can result in an instance of higher energy within the stress plane (9). A crack is initiated If the force applied exceeds the strength of the tooth structure fracture resistance (10). Cracks in teeth usually occur in a mesio-distal direction in the crown, and then propagate longitudinally due the direction of the load applied during mastication or maximum intercuspation (11). Cracks can extend to the cemento-enamel junction (CEJ), involve just an individual cusp or extend into the root (11).

Peri-Cervical Dentin

PCD is dentin roughly 4mm apical and coronal to the crestal bone (12). The conservation of PCD is critical because while the crown is restorable and root tips can be amputated, the PCD is non restorable (12). In addition, the PCD is directly related to fracture resistance and long-term retention of teeth (13,14). Current literature suggests that the main cause of root-filled teeth extraction is structural or restorative failure, while failures of true endodontic origin are least reported (15,16).

Minimally Invasive Endodontics

A growing number of clinicians are following the trend toward minimally invasive endodontics. This shift includes techniques from conservative access preparations to minimally invasive file systems that conserve PCD and radicular dentin (17). However, the benefit of such a shift is disputed. Some studies claim that minimally invasive accesses and file systems have no benefit to the fracture resistance of a tooth

(18–20), others conclude that a significant benefit can be observed (4,7,21). While these studies provide valuable insight on stress concentrations of endodontically treated teeth, none evaluated the effect of minimally invasive endodontics on the propagation of longitudinal cracks. Studying crack propagation in teeth is a difficult endeavor, which is also why it is one of the American Association of Endodontists' top research priorities. Based on current technology, there is no way to visualize or assess the extent and size of a crack *in vivo*. Once a tooth is extracted, it can be evaluated for cracks and fractures, but the extracted tooth does not provide insight into the etiology of the crack and what factors led to its propagation in real time.

Minimally Invasive Instrumentation

Contemporary endodontics exhibit two contrasting instrumentation strategies used by clinicians. These strategies include minimally tapered regressive instrumentation (Minimally Invasive) as compared to a progressively tapered shape. The goal of mechanical instrumentation as described by Schilder, is to clean root canal spaces of their organic remnants which could serve as a substrate for bacterial growth and shape them to receive a three-dimensional fill (22). There is a significant body of literature that suggests larger apical diameters and tapers allow for improved removal of debris and deeper penetration of the irrigant leading to a decrease in bacterial contamination (23–25). In contrast, a study concluded that no difference in bacterial reduction was noted in between the size 25 and 40 file groups after instrumentation (26). The goal of minimally invasive instrumentation is to conserve peri-cervical and root dentin by limiting the maximum flute diameter and employing regressive tapers (27). Improved nickel-titanium metallurgy, manufacturing, obturation materials, and irrigation protocols have made it

possible to adopt less invasive approaches in endodontic instrumentation (27). However, regardless of which instrumentation technique is employed, it is not possible to completely rid the canal of microorganisms by mechanical instrumentation alone (28).

Finite Element Analysis

The finite element method (FEM) is a mathematical tool used to find approximate solutions to differential equations by dividing a geometric structure into smaller elements connected at nodes (29). This method underlies finite element analysis (FEA), which allows for a three-dimensional (3D) examination of complex geometric interactions, reducing the need for physical prototypes and providing more accurate results through computer simulation (29). FEA also offers the ability to visualize stress forces at different points of the object being analyzed. In the human body, differences in bone quality, density, and shape have a significant impact on tooth strength and the formation of cracks and fractures. The finite element method has been used for nearly three decades to study various aspects of dentistry (6,7,19–21,30). Studies have utilized FEA to assess stress distribution in dental prosthetics and teeth during occlusal loading (30), stress on various thicknesses of mineral trioxide aggregate placed on different widths of pulp perforations (6), compare residual tooth strength and stress distribution of a mandibular molar prepared with different variable tapered file systems (7).

Previous studies of stress distribution on cracked teeth with different access openings have had limitations, including the lack of incorporation of the periodontal ligament and bone modeling in the FEA (5). The benefits of using FEA include repeatability, absence of ethical concerns commonly associated with human-based studies, and the ability to modify study design as needed to improve simulation of oral

biomechanics. However, limitations still exist in previous model designs, such as simplified assumptions about modeling geometry, loading, boundary conditions, and material properties that can significantly affect analytical results.

MATERIALS AND METHODS

Sample Preparations

Two identical 3-dimensionally printed mandibular plastic molars (tooth #19) were used in this study (Endo 3DP; Acadental, Lenexa, KS). Both teeth were printed with a conventional endodontic access. The teeth were then inserted into ModuPRO carriers (Acadental) and inserted into the ModuPRO manikin (Acadental). A glide path up to a 15 K-file (Roydent, Johnson City, TN) was achieved in both of the teeth and the working length measurement was established with a radiograph 0.5 mm short of the radiographic apex. Group 1 was instrumented with ProTaper Gold to F2 (25/0.08v) in the mesial canals and F3 (30/0.09v) in the distal canals as described in the manufacturers protocol. Group 2 was instrumented with the TruNatomy system to a primary 26/0.04v in the mesial canals and 36/0.03v in the distal canals according to the manufacturer's protocol. Following instrumentation, the canals were irrigated with saline, dried with the corresponding paper points and obturated with EndoSequence BC Sealer (Brasseler USA, Savannah, GA), gutta-percha, and warm vertical compaction. Following obturation the access restoration was restored with composite. All procedures were completed in a manikin using a microscope to simulate clinical treatment. After the RCT procedures were completed, all teeth were digitized using a high-resolution micro-computed tomographic scan to create 3-D models and stereolithographic reconstructions for FEA.

Micro CT and Meshing

A micro-CT scan and stereolithographic reconstruction of teeth were completed using a GOM computed tomographic scanner at 25-mmol/L voxel size, 150-kV target X-ray voltage, 40 W X-ray target power, exposure time of 1500 milliseconds, 750



exposures, and GOM Inspect software (Fig.1). A numerical approach based on the Finite Element Method using the commercial software ANSYS is used to study the crack growth behavior of a root canal treated teeth subjected to a mastication loading of 60 MPa applied on four circular spots of a total area around 4 mm² (247 Newtons), (Fig.2). The crack growth is evaluated based on the Paris Law model $\frac{da}{dN} = C (\Delta k)^m$. The model describes the relationship between the crack growth rate ($\frac{da}{dN}$) and the induced range of stress intensity factor (Δk) where, a is the crack length, N is the number of cycles, C and m are material properties and k the stress intensity factor.

Geometry Building

The 3D Computer-aided design (CAD) models of the molar outer surface, inner pulp cavity, various crown/canal preparation shapes, and filling material bulk were created (Fig. 3). The main segmented data for the molar geometry in its intact and prepared conditions were generated from a micro-CT acquisition using a GOM (Braunschweig, Germany) computed tomographic scanner. The collected data was merged into STL files for further polygon decimation, smoothening, and refinement on Geomagic software (3D systems) (Fig. 4). Manual patches were generated and NURBS surfaces fitted and exported in IGES format for additional manipulations on Solidworks software (Dassault systèmes). The planned manipulations were; demarcating dentine and enamel bodies, performing Boolean operations to hollow the dentine body using the inner surfaces representative of various crown/canal preparations, virtual development and positioning of the crack in the crown, building the composite filling for the treatment scenarios to be addressed, in-context reconstruction of the periodontal ligament with a uniform thickness of 0.2mm, intuitive generation of a mandibular bone segment



consisting of cancellous bone and surrounding cortical layer, prompt demarcation of the areas characteristic of the boundary conditions and loadings to be used in the simulation phase. The crack was simulated at the distal marginal ridge extending horizontally to the distal occlusal cavo-surface margin and apically 2mm above the CEJ (Fig. 5). The values for the structural properties of the materials incorporated into the study were from previously published data (5–7,19,20,29,30) (Tables 1-6).

Table 1: *Structural Properties of Enamel.*



 **Enamel** 

Structural	
▼ Isotropic Elasticity	
Derive from	Young's Modulus and Poisson's Ratio
Young's Modulus	41000 MPa
Poisson's Ratio	0.31
Bulk Modulus	35965 MPa
Shear Modulus	15649 MPa
▼ Paris' Law	
Reference Units (Length, Force)	mm, tonne mm s ⁻²
Material Constant C	2.452e-15
Material Constant m	7.7


Table 2: *Structural Properties of Cancellous Bone.*

 **Cancellous Bone** 

Structural	
▼ Isotropic Elasticity	
Derive from	Young's Modulus and Poisson's Ratio
Young's Modulus	1370 MPa
Poisson's Ratio	0.3
Bulk Modulus	1141.7 MPa
Shear Modulus	526.92 MPa

Table 3: Structural Properties of Composite.



Composite	
Structural	
▼ Isotropic Elasticity	
Derive from	Young's Modulus and Poisson's Ratio
Young's Modulus	16400 MPa
Poisson's Ratio	0.28
Bulk Modulus	12424 MPa
Shear Modulus	6406.3 MPa
▼ Paris' Law	
Reference Units (Length, Force)	mm, tonne mm s ⁻²
Material Constant C	2.452e-15
Material Constant m	7.7

Table 4: Structural Properties of Cortical Bone.



Cortical Bone	
Structural	
▼ Isotropic Elasticity	
Derive from	Young's Modulus and Poisson's Ratio
Young's Modulus	13700 MPa
Poisson's Ratio	0.3
Bulk Modulus	11417 MPa
Shear Modulus	5269.2 MPa

Table 5: Structural Properties of the Periodontal Ligament.

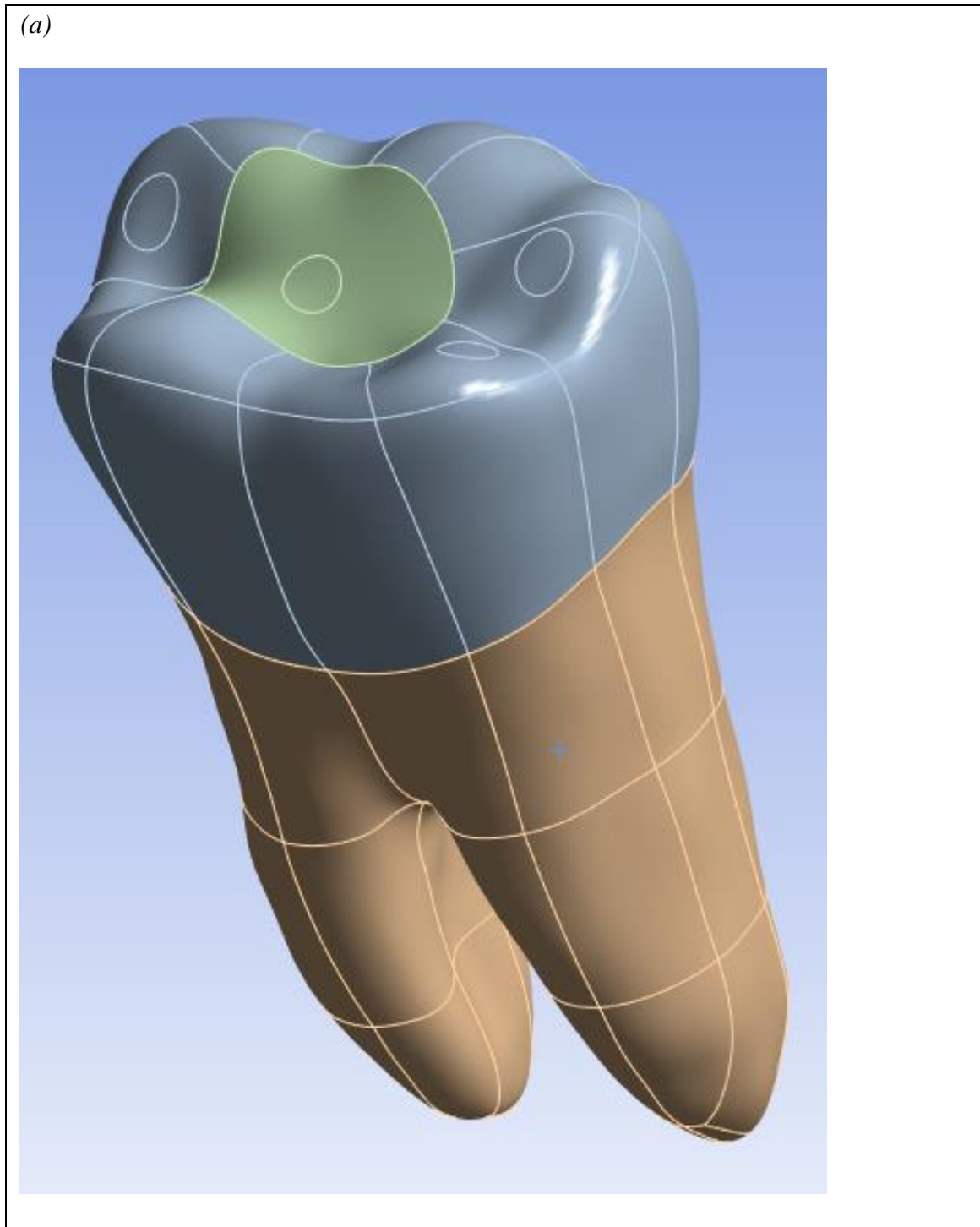


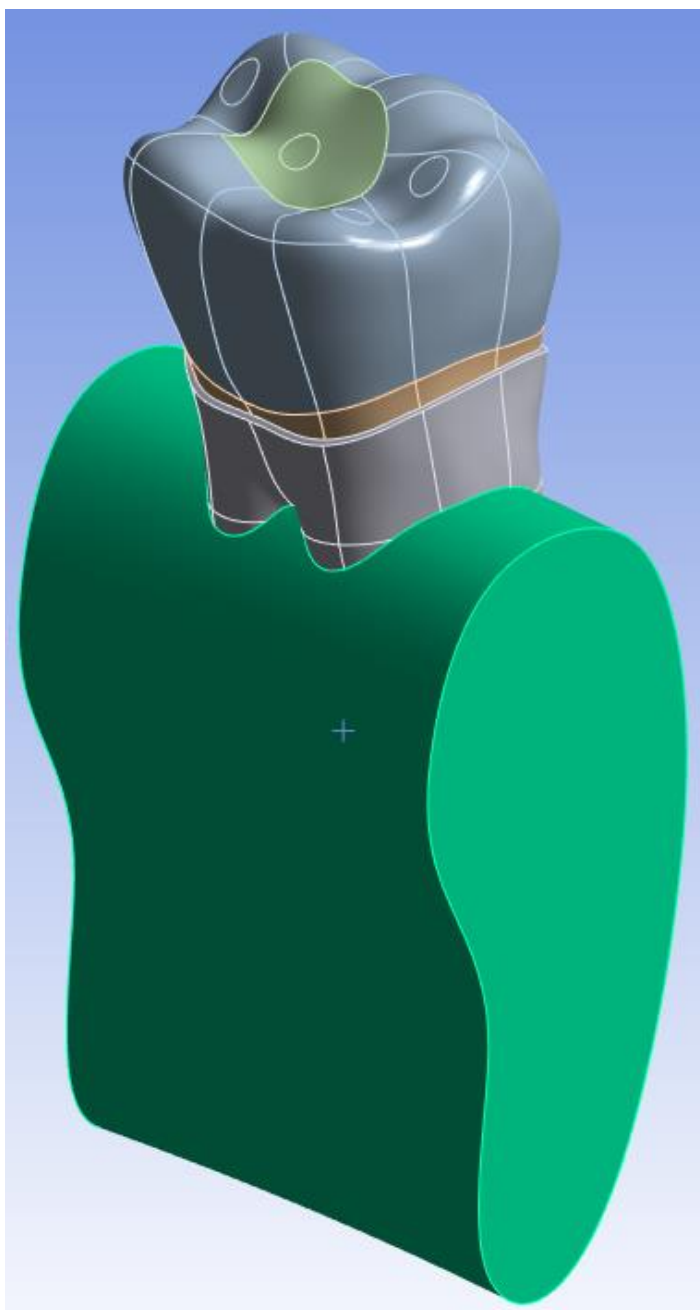
PLD	
Structural	
▼ Isotropic Elasticity	
Derive from	Young's Modulus and Poisson's Ratio
Young's Modulus	68.9 MPa
Poisson's Ratio	0.45
Bulk Modulus	229.67 MPa
Shear Modulus	23.759 MPa

Table 6: *Structural Properties of Dentin.***Dentin**

Structural		▼
▼ Isotropic Elasticity		
Derive from	Young's Modulus and Poisson's Ratio	
Young's Modulus	18600 MPa	
Poisson's Ratio	0.31	
Bulk Modulus	16316 MPa	
Shear Modulus	7099.2 MPa	
▼ Paris' Law		
Reference Units (Length, Force)	mm, tonne mm s ⁻²	
Material Constant C	4.5205e-24	
Material Constant m	8.76	

Figure 1: (a) Stereolithographic reconstruction of the scanned mandibular molar, with delineated enamel, composite filling, root dentin, (b) simulated periodontium added to reconstruction, and (c) Occlusal view of reconstructed mandibular molar.



(b)

(c)

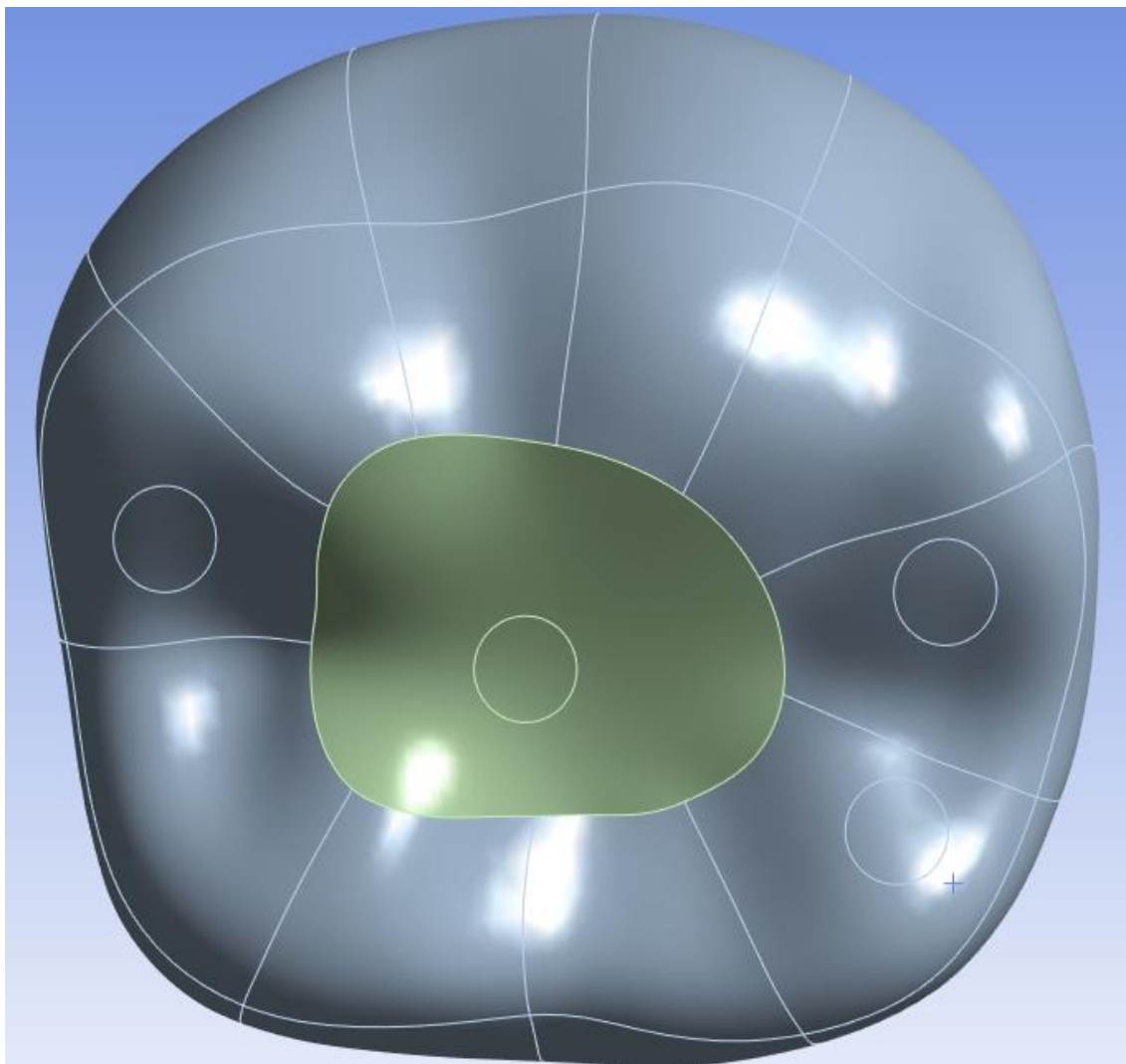
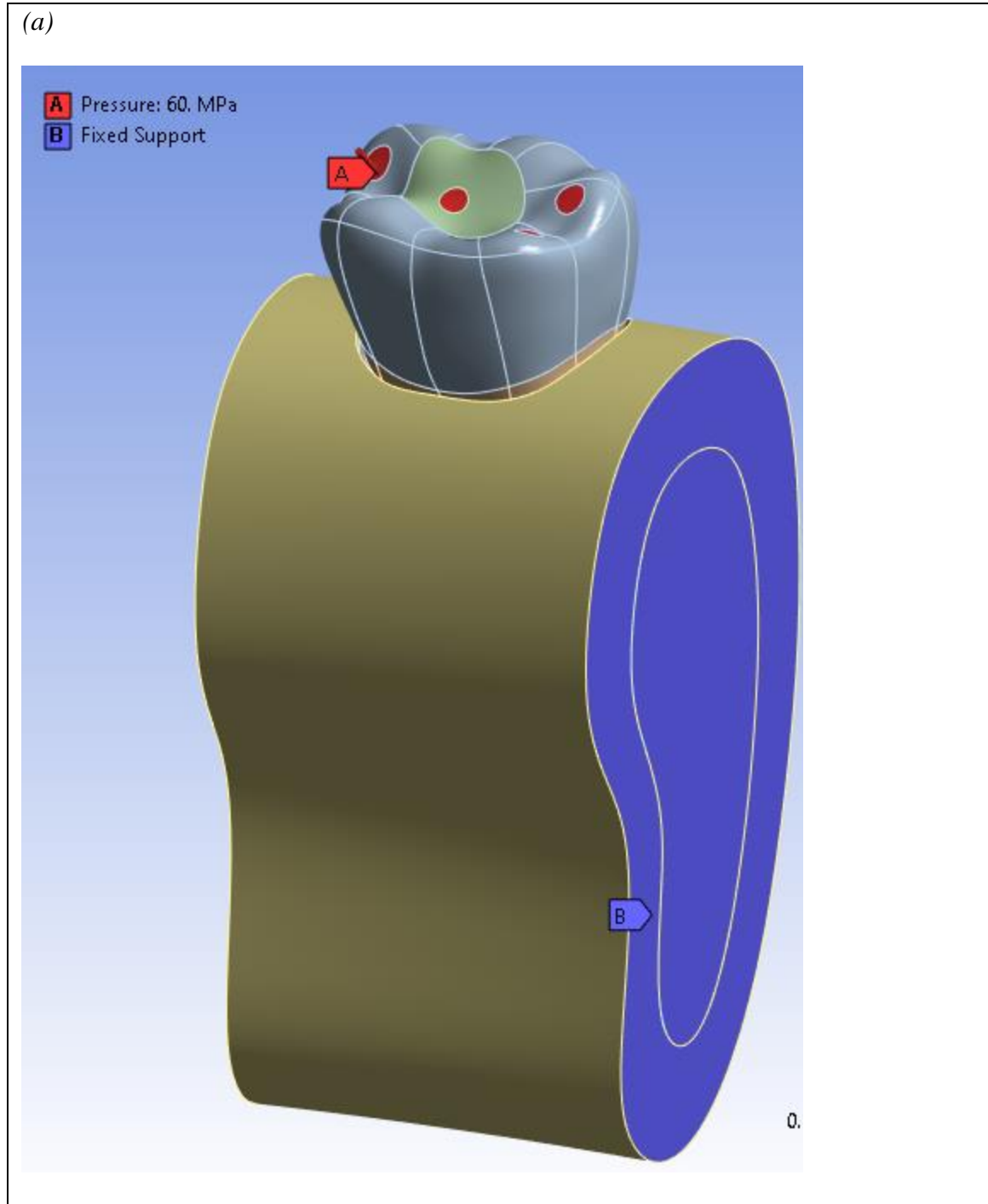


Figure 2: Mastication Load distribution on occlusal surface.



(b)

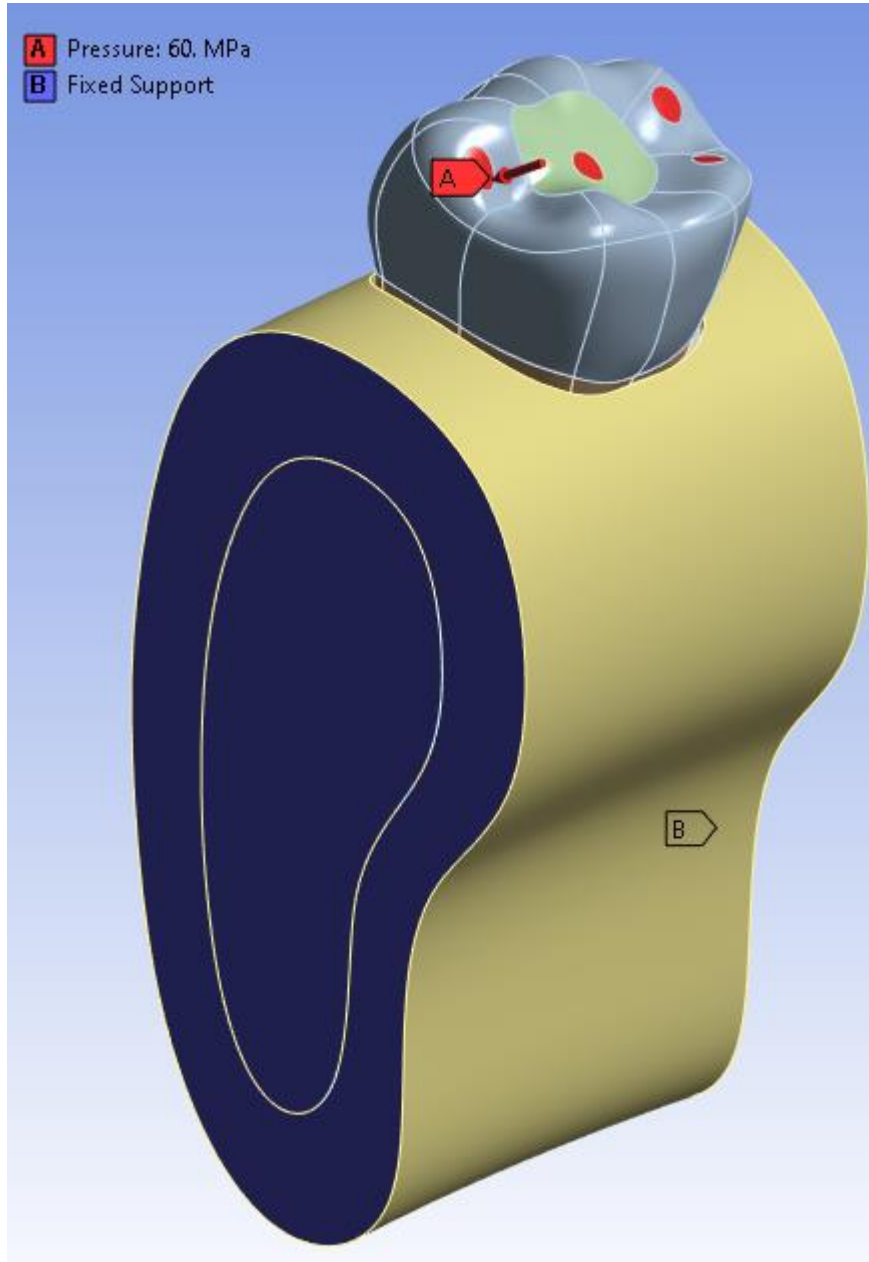
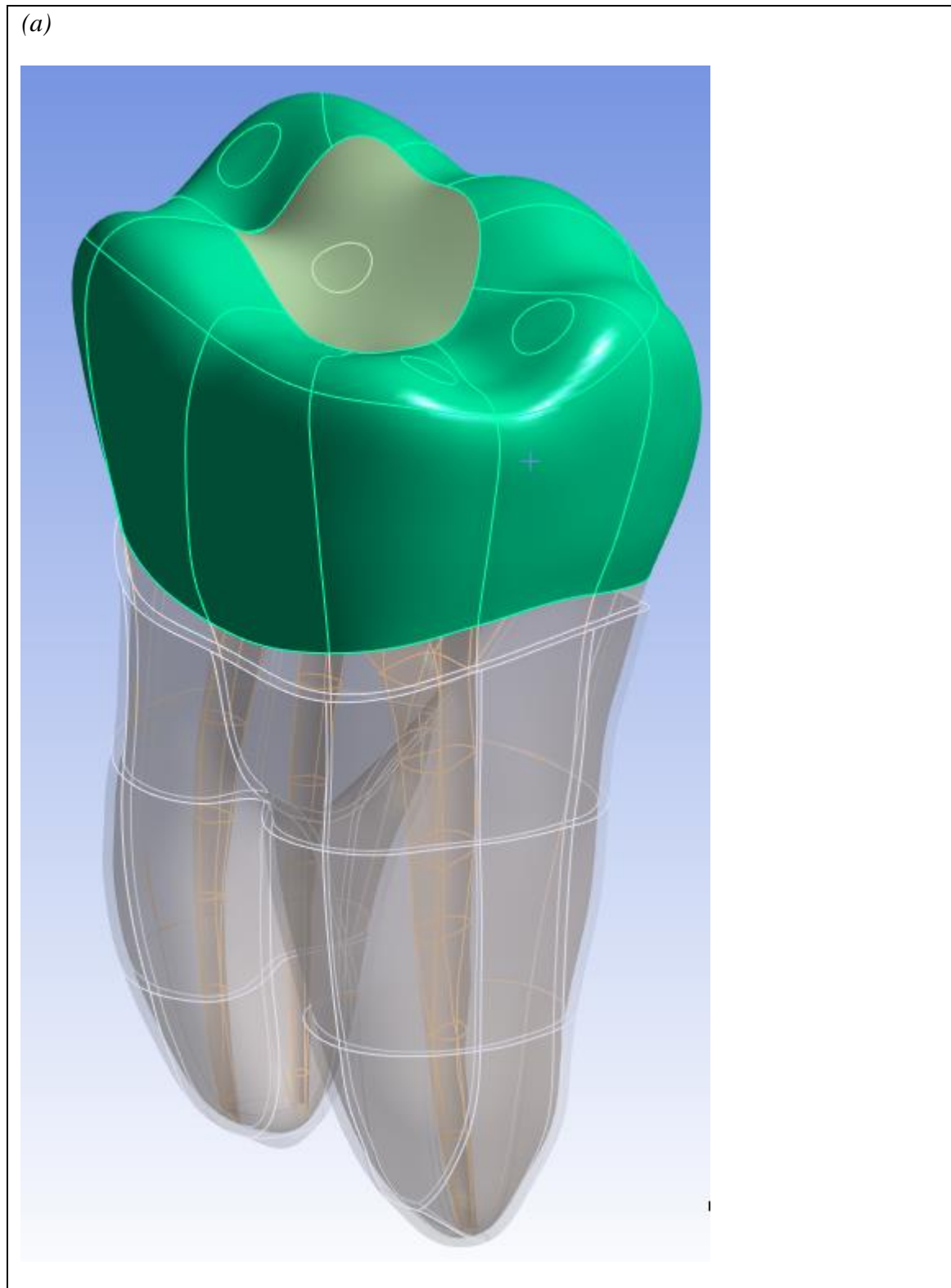


Figure 3: 3D CAD models of the molar outer surface (a), (b) access and inner pulp cavity, and crown/canal preparation shapes.



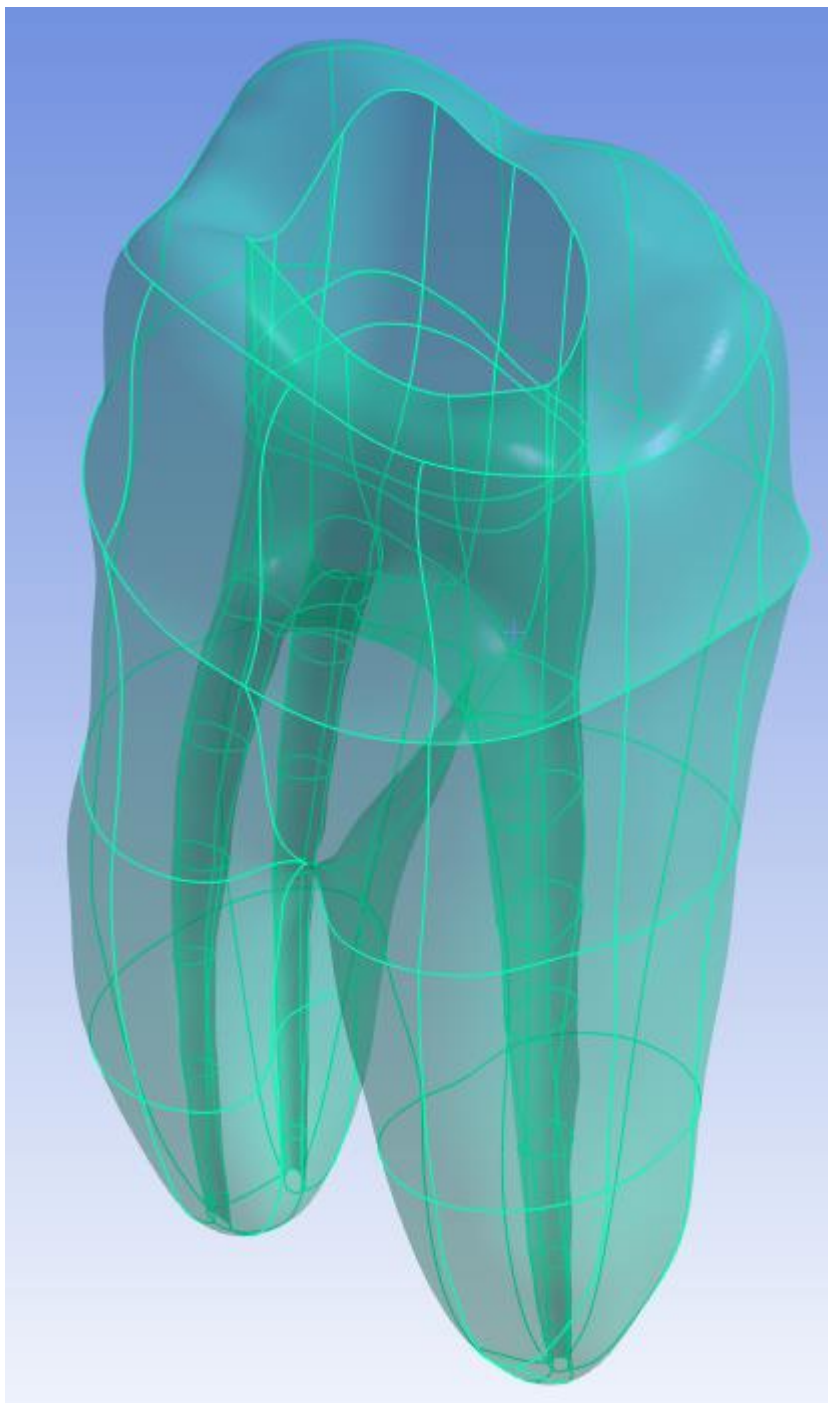
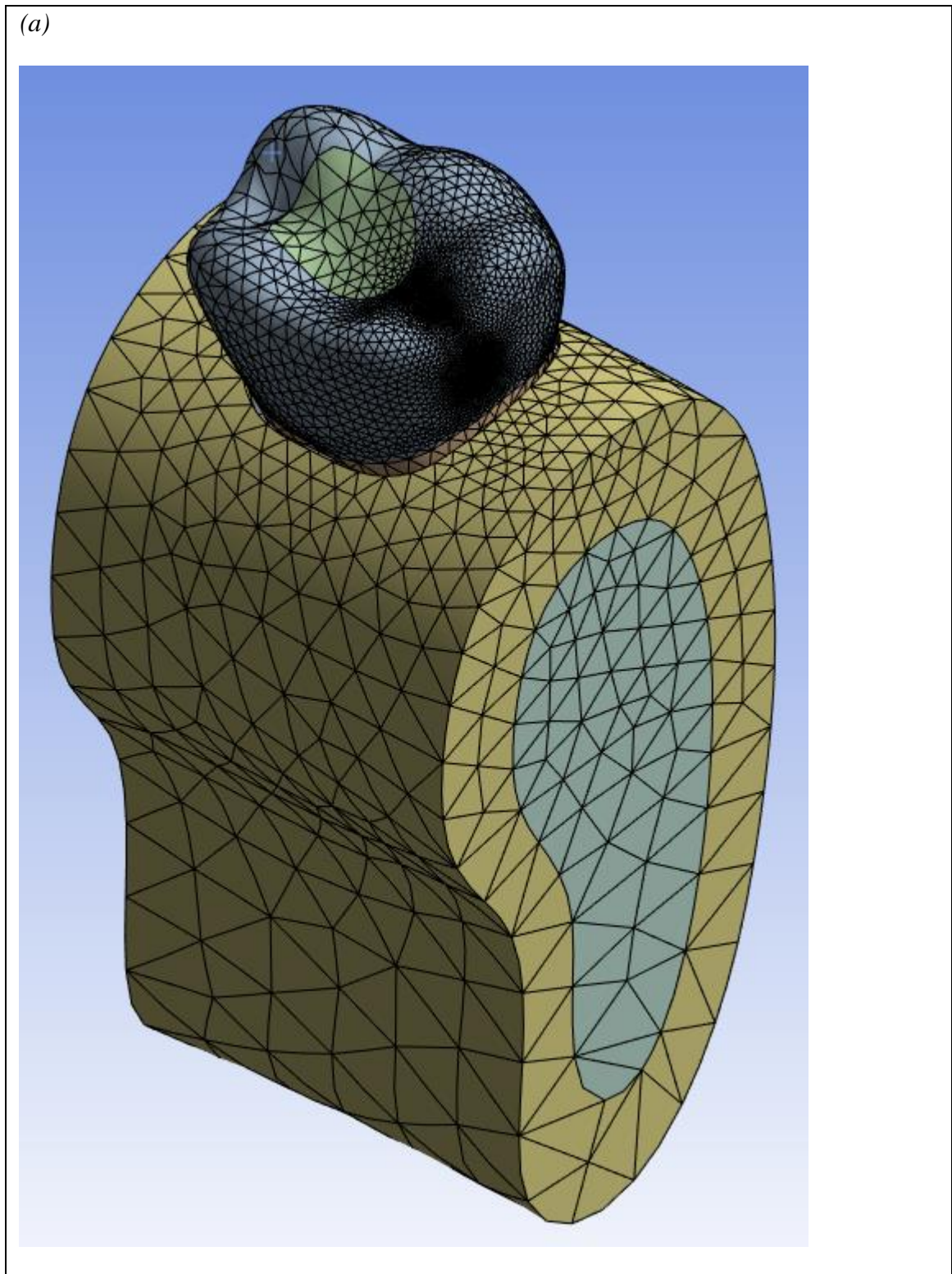
(b)

Figure 4: Polygon decimation, smoothing, and refinement on Geomagic software (3D systems)



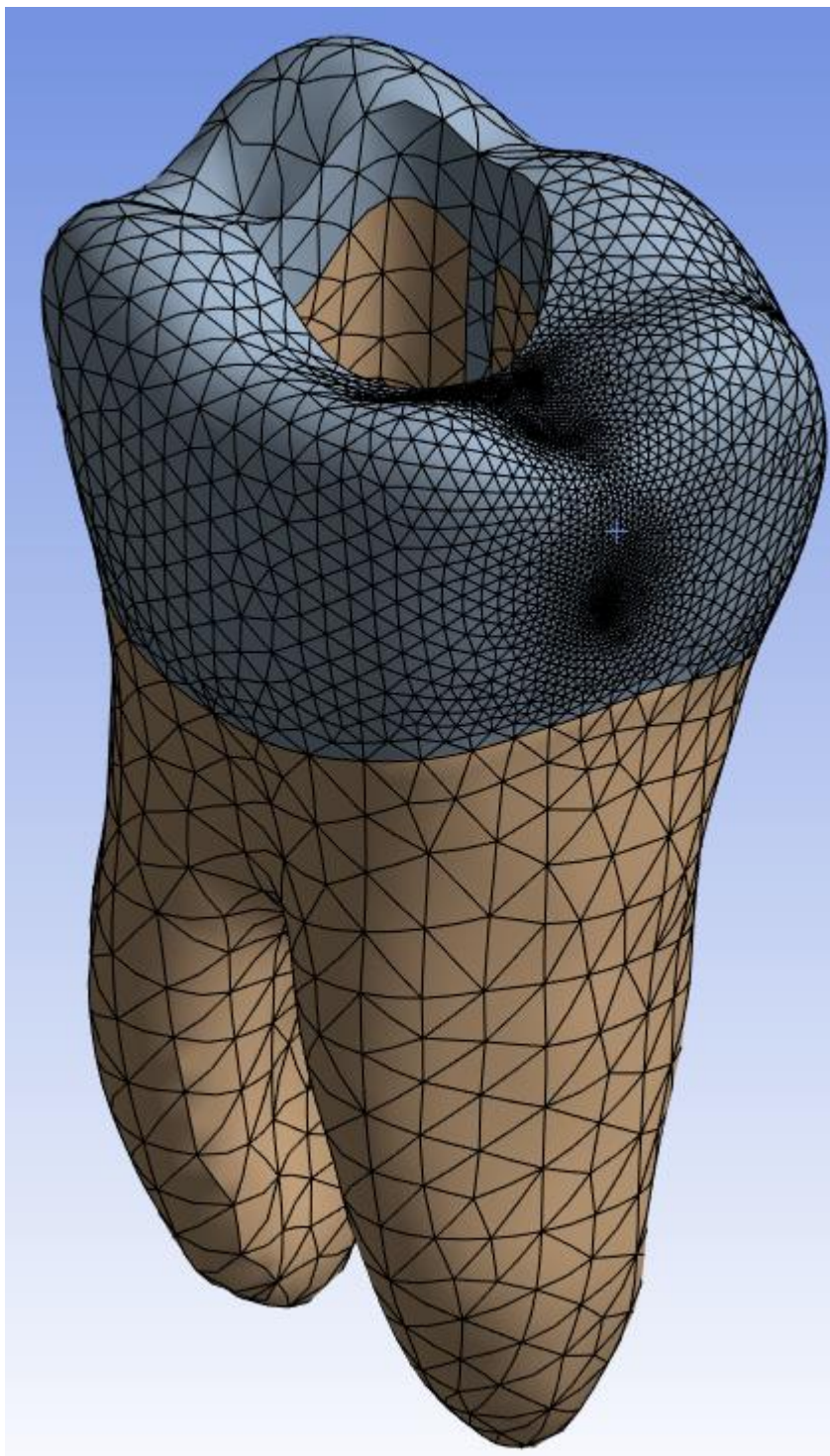
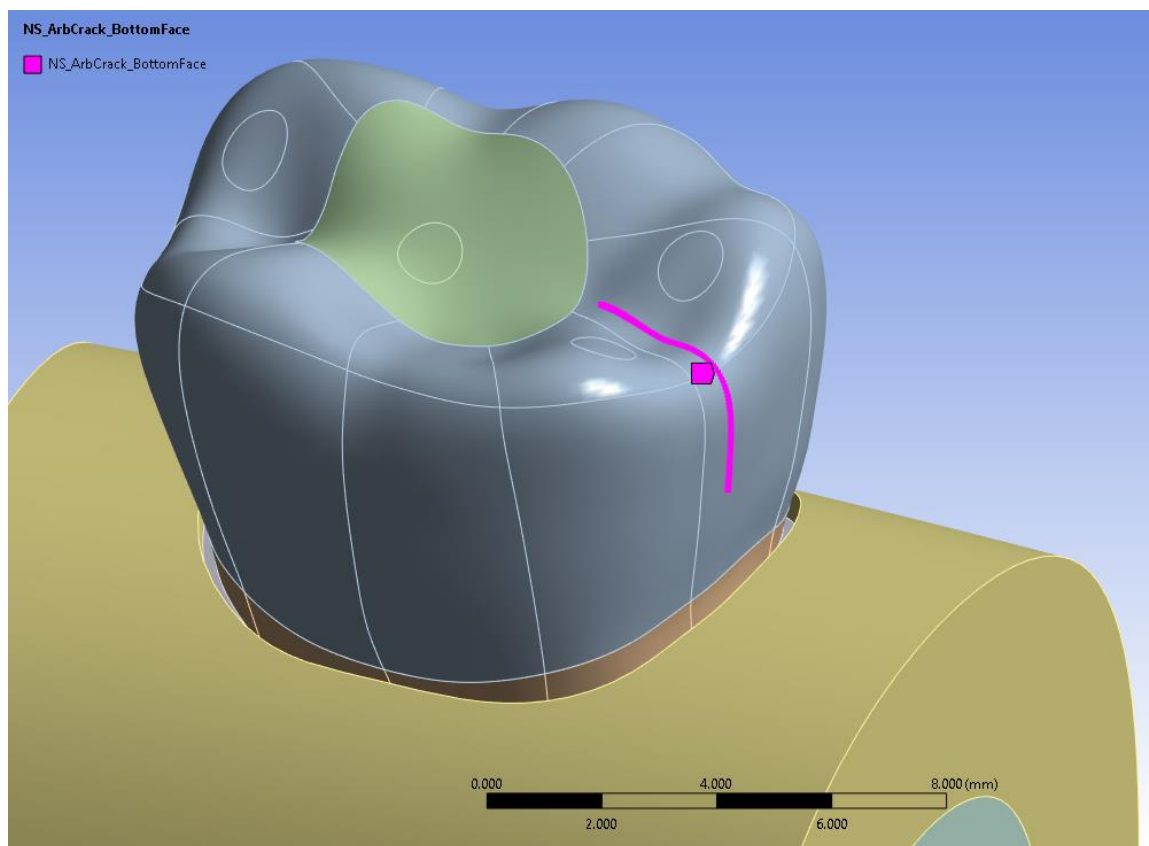
(b)

Figure 5: Initial crack simulation and position at the distal marginal ridge extending horizontally to the distal occlusal cavo-surface margin and apically 2mm above the CEJ



Results

The results demonstrated the extension of the simulated crack over the amount of mastication cycles. Each mastication cycle was simulated as a period in sinusoidal cycle with a constant amplitude corresponding to the application of 247 N of force distributed evenly through the four contact points. In both groups, the crack started propagating around 40,000 mastication cycles (Fig. 6, Fig 7). Group 1 which was instrumented with Protaper Gold, had 0.5mm of crack propagation at 60,218,000 mastication cycles (Fig. 6, Fig. 8). Group 2 which was instrumented with TruNatomy, had 0.5mm of crack propagation at 10,042,000 cycles (Fig. 7, Fig 9). After 60,461,000 cycles, the computer used in the study was unable to generate more data due a lack of processing power.

Figure 6: Group 1 crack propagation in mm over number of mastication cycles.

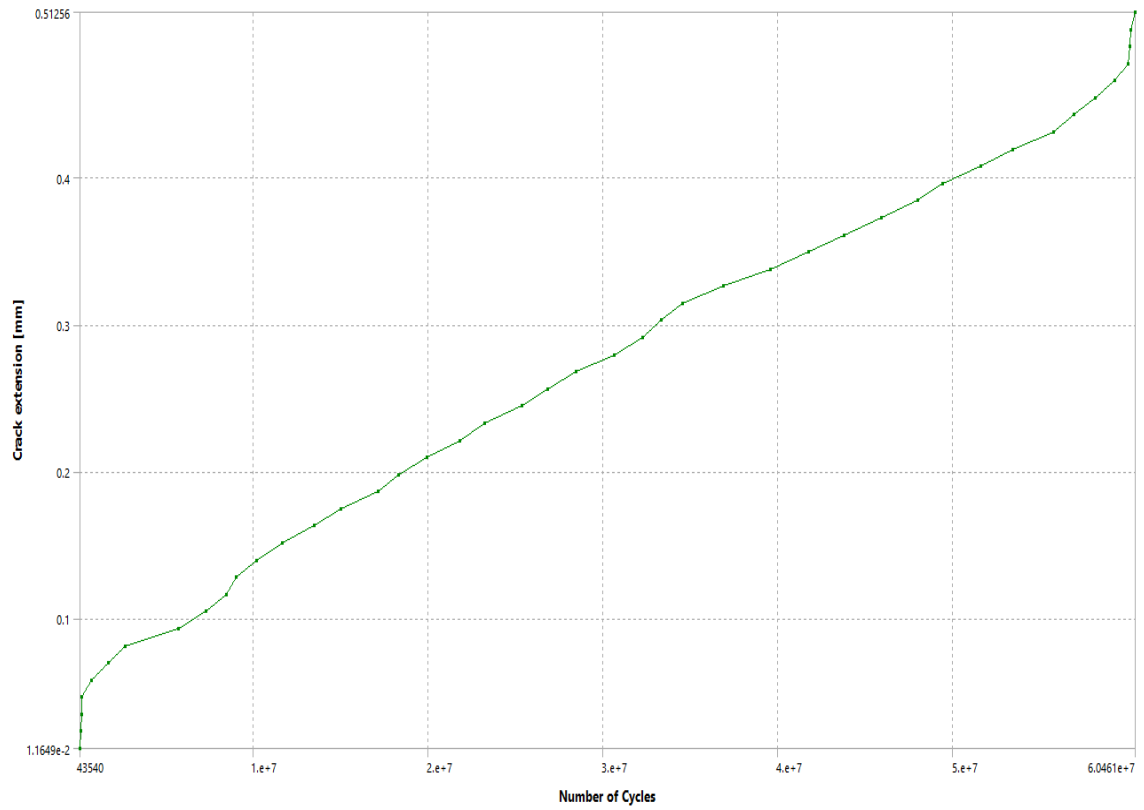


Figure 7: Group 2 crack propagation in mm over number of mastication cycles.

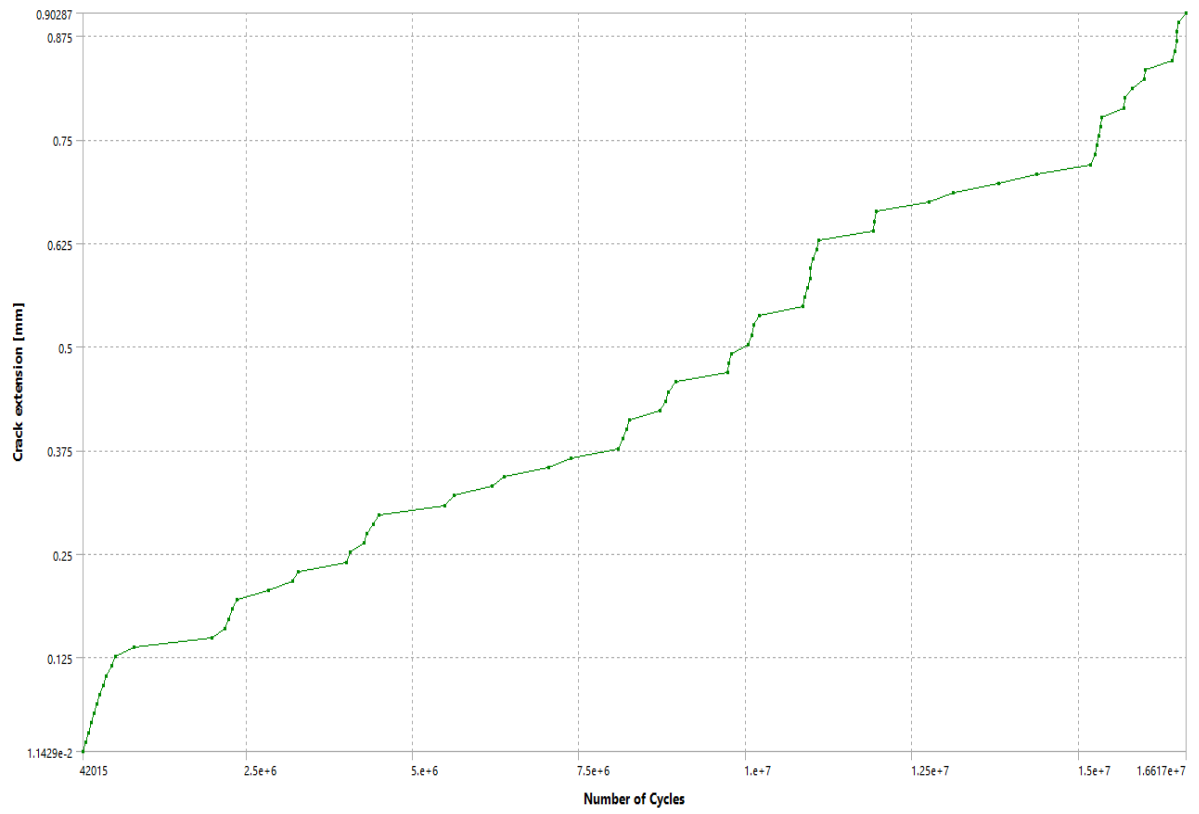


Figure 8: 3D visualization of group 1 Crack propagation

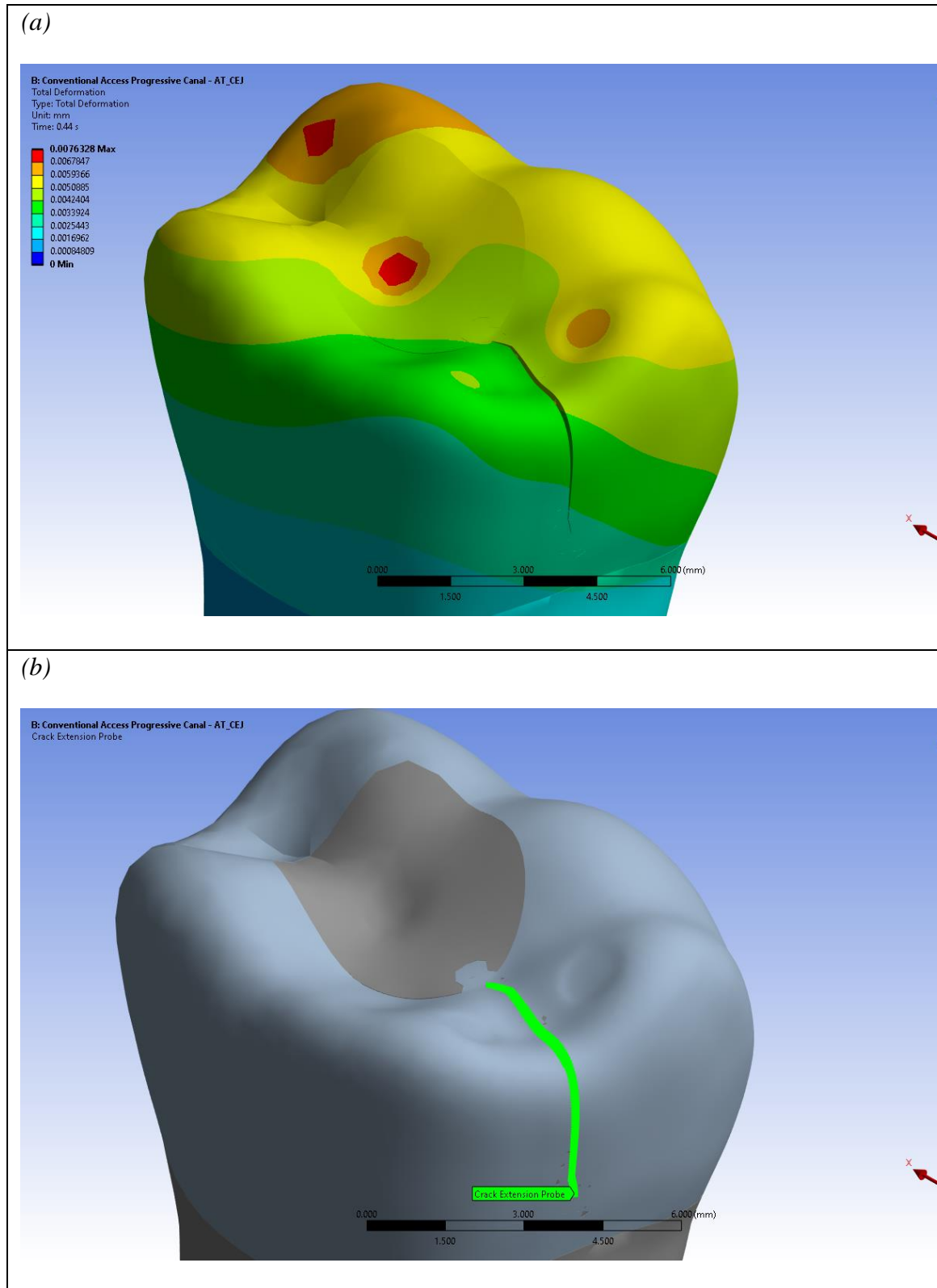
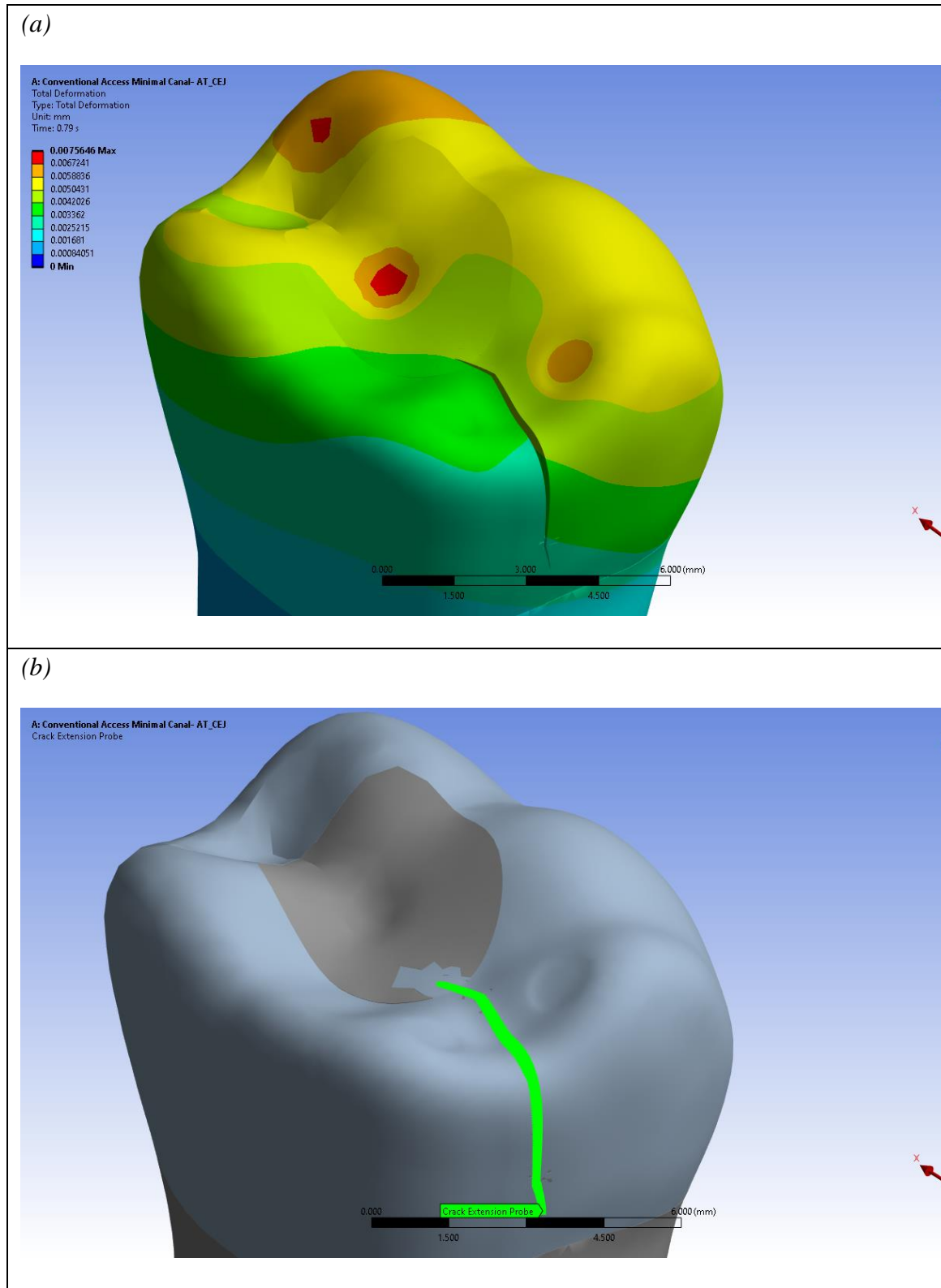


Figure 9: 3D visualization of group 2 Crack propagation



DISCUSSION

The list of FEA studies in dentistry is extensive however the clinical application is questionable due to the limitations with FEA. This study sought to overcome some of the limitations of FEA studies by creating a more realistic 3D model and occlusal load simulation. A mandibular molar was used in the simulation because it is the most commonly fractured endodontically treated tooth (7,31,32). The tooth was mounted in a simulation lab mannequin/typodont with a rubber dam, instrumented with rotary files, obturated and restored to simulate a real patient scenario. A 4-point contact system as described in Okeson's textbook was used to simulate clinical occlusal contacts (33). Finally, to mimic the load experienced during oral mastication, 250 N of cyclic load was distributed through the 4 contact points (34,35).

FEA has proven to be a valid analytical tool for evaluating stress and crack propagation in computer generated models. FEA allows for standardization among experimental samples that cannot be obtained using in vivo research. In this study the propagation of cracks in teeth was analyzed via a novel FEA method. The objective of this study was to investigate the effect of PCD conservation during root canal treatment on the longitudinal propagation of cracks, utilizing the Finite Element Method.

The aim of minimally invasive endodontics is to decrease the removal of tooth structure during root canal therapy. The trend towards minimally invasive endodontics is not only being adopted by an increasing number of clinicians, but also dental manufacturers. TruNatomy, a minimally invasive file system recently developed, boasts a

MFD of 0.8mm in comparison to PTG's 1.2mm. At first glance .4mm decrease seems negligible but that is a 33% difference in the MFD which will theoretically yield in more conservation of PCD, depending on the original canal taper and apical size. A recent study compared the impact of TruNatomy and PTG Instruments on the preservation of the PCD found that a higher mean percentage removal of dentin was observed at the coronal level of mesial roots of mandibular molars prepared with PTG compared with TruNatomy (36). It can also be theorized that the mean percentage removal of PCD will be greater in calcified teeth due to presence of more secondary and tertiary dentin.

The effect of PCD removal on fracture resistance has been researched previously but no published studies have evaluated the effect PCD conservation on the longitudinal propagation of cracks. In the current study, a crack was simulated on the occlusal surface of the digitized tooth model. Since cracks occur most frequently in a mesio-distal direction (11), the crack was simulated extending mesiodistally on the model. The crack originated at the distal marginal ridge extending horizontally to the distal occlusal cavo-surface margin and apically 2mm above the CEJ. The longitudinal extent of the crack was intentionally limited to 2mm above the CEJ, occlusal to the PCD, to assess if the crack propagates to and apical to CEJ based on the file system used.

After 60,461,000 cycles the computer which ran the FEA was not able to process more cycles and continued to crash after multiple attempts. Running the FEA for stress concentrations is a demanding challenge for the computer, and with the added complexity of estimating crack propagation, it overloads the computer processor which leads the software to crash. To estimate crack propagation for a larger number of cycles, the FEA will have to be run on a supercomputer with larger processing power and RAM.

The null hypothesis was rejected given that the result of this study suggests that mandibular molars instrumented with PTG will have less crack propagation for the same amount of mastication cycles as compared with molars instrumented with TruNatomy. Multiple studies have suggested that excess loss of PCD can decrease fracture resistance of a tooth (7,10,18,19,21) and instrumentation with PTG yields a greater loss of PCD as compared with TruNatomy. In contrast, some studies claim that minimally invasive accesses and loss of PCD have no benefit to the fracture resistance of a tooth (18–20,37). In the present study, root canal instrumentation with a more conservative file system led to higher rate in crack propagation. One explanation for this could be due to the higher stiffness in teeth instrumented with TruNatomy, due to an increased amount of preserved tooth structure. While there will always be limitations associated with FEA studies, the benefits will continue to grow as scanning and analysis methods are improved in future software updates. Improvements in the software could include a more realistic mastication cycle which simulates Posselt's envelope of motion, adding soft tissue boundaries with physical properties and optimized programming to enable longer FEA cycles for readily available computers. Future FEA studies are needed which utilize updated clinical boundaries and technology to predict the crack propagation of endodontically treated teeth more accurately.

CONCLUSIONS

Within the limitations of this study, it can be concluded that the crack propagation rate was less with mandibular molars instrumented with PTG compared to TruNatomy. The propagation of the simulated crack for both PTG and TruNatomy initiated around 40,000 loading cycles. The PTG instrumented tooth had 0.5mm of crack propagation at 60,218,000 mastication cycles compared to 10,042,000 cycles for TruNatomy. After 60,461,000 cycles, the computer used in the study was not able to generate more data due a lack of processing power. To simulate a large amount of mastication cycles, a computer with more processing power is needed.

BIBLIOGRAPHY

1. Nosrat A, Yu P, Verma P, Dianat O, Wu D, Fouad AF. Was the Coronavirus Disease 2019 Pandemic Associated with an Increased Rate of Cracked Teeth? *J Endod.* 2022;48(10):1241–7.
2. Hilton T FJ. Cracked Teeth Registry. National Dental PBRN Western Regional Meeting. 2013
3. Hylander WL. Mandibular function in *Galago crassicaudatus* and *Macaca fascicularis*: an in vivo approach to stress analysis of the mandible. *J Morphol.* 1979;159(2):253–96.
4. Bier CAS, Shemesh H, Tanomaru-Filho M, Wesselink PR, Wu MK. The Ability of Different Nickel-Titanium Rotary Instruments To Induce Dentinal Damage During Canal Preparation. *J Endod.* 2009 1;35(2):236–8.
5. Mamoun JS, Napoletano D. Cracked tooth diagnosis and treatment: An alternative paradigm. *Eur J Dent.* 2015;9(2):293–303.
6. Kishen A. Mechanisms and risk factors for fracture predilection in endodontically treated teeth. *Endod Topics.* 2006;13(1):57–83.
7. Clark DJ, Sheets CG, Paquette JM. Definitive diagnosis of early enamel and dentin cracks based on microscopic evaluation. *J Esthet Restor Dent.* 2003;15(7):391–401.
8. Clark D, Khademi J. Modern Molar Endodontic Access and Directed Dentin Conservation. *Dent Clin North Am.* 2010;54(2):249–73.
9. Goto Y, Nicholls JJ, Phillips KM, Junge T. Fatigue resistance of endodontically treated teeth restored with three dowel-and-core systems. *Journal of Prosthetic Dentistry.* 2005;93(1):45–50.
10. Kutesa-Mutebi A, Osman YI. Effect of the ferrule on fracture resistance of teeth restored with prefabricated posts and composite cores. *Afr Health Sci.* 2004;4(2):131.
11. Ng YL, Mann V, Gulabivala K. A prospective study of the factors affecting outcomes of non-surgical root canal treatment: part 2: tooth survival. *Int Endod J.* 2011;44(7):610–25.
12. Vire DE. Failure of endodontically treated teeth: classification and evaluation. *J Endod.* 1991;17(7):338–42.

13. Mathew ST, Rajan JS. Minimally invasive endodontics. *Journal of Dentistry and Oral Hygiene*. 2014;6(4):36–8.
14. Barbosa AFA, Silva EJNL, Coelho BP, Ferreira CMA, Lima CO, Sassone LM. The influence of endodontic access cavity design on the efficacy of canal instrumentation, microbial reduction, root canal filling and fracture resistance in mandibular molars. *Int Endod J*. 2020;53(12):1666–79.
15. Nawar NN, Kataia M, Omar N, Kataia EM, Kim HC. Biomechanical Behavior and Life Span of Maxillary Molar According to the Access Preparation and Pericervical Dentin Preservation: Finite Element Analysis. *J Endod*. 2022;48(7):902–8.
16. Jiang Q, Huang Y, Tu X, Li Z, He Y, Yang X. Biomechanical Properties of First Maxillary Molars with Different Endodontic Cavities: A Finite Element Analysis. *J Endod*. 2018;44:1283–8.
17. Liu Y, Liu H, Fan B. Influence of Cavity Designs on Fracture Behavior of a Mandibular First Premolar with a Severely Curved h-shaped Canal. *J Endod*. 2021;47(6):1000–6.
18. Smoljan M, Hussein MO, Guentsch A, Ibrahim M. Influence of Progressive Versus Minimal Canal Preparations on the Fracture Resistance of Mandibular Molars: A 3-Dimensional Finite Element Analysis. *J Endod*. 2021;47(6):932–8.
19. Schilder H - 1974 - Cleaning and Shaping The Root Canal | PDF.
20. Weiger R, Bartha T, Kalwitzki M, Löst C. A clinical method to determine the optimal apical preparation size. Part I. *Oral Surgery, Oral Medicine, Oral Pathology, Oral Radiology, and Endodontology*. 2006;102(5):686–91.
21. Clark Dalton B, Orstavik D, Phillips C, Pettiette M, Trope M. Bacterial reduction with nickel-titanium rotary instrumentation. *J Endod*. 1998;24(11):763–7.
22. Salzgeber RM, Brilliant JD. An in vivo evaluation of the penetration of an irrigating solution in root canals. *J Endod*. 1977;3(10):394–8.
23. Yared GM, Bou Dagher FE. Influence of apical enlargement on bacterial infection during treatment of apical periodontitis. *J Endod*. 1994;20(11):535–7.
24. Gluskin AH, Peters CI, Peters OA. Minimally invasive endodontics: challenging prevailing paradigms. *British Dental Journal* 2014 216:6. 2014;216(6):347–53.
25. JF S, MC A, PF G, RC F, CJ D. Histological evaluation of the effectiveness of five instrumentation techniques for cleaning the apical third of root canals. *J Endod*. 1997;23(8):499–502.

26. Trivedi S. Finite element analysis: A boon to dentistry. *J Oral Biol Craniofac Res.* 2014;4(3):200.
27. Ozkurt-Kayahan Z, Turgut B, Akin H, Kayahan MB, Kazazoglu E. A 3D finite element analysis of stress distribution on different thicknesses of mineral trioxide aggregate applied on various sizes of pulp perforation. *Clin Oral Investig.* 2020;24(10):3477–83.
28. Ramakrishaniah R, Al Kheraif AA, Elsharawy MA, Alsaleh AK, Ismail Mohamed KM, Rehman IU. A comparative finite elemental analysis of glass abutment supported and unsupported cantilever fixed partial denture. *Dent Mater.* 2015;31(5):514–21.
29. Allen C, Meyer CA, Yoo E, Vargas JA, Liu Y, Jalali P. Stress distribution in a tooth treated through minimally invasive access compared to one treated through traditional access: A finite element analysis study. *J Conserv Dent.* 2018;21(5):505.
30. Cohen S, Blanco L, Berman L. Vertical root fractures: Clinical and radiographic diagnosis. *The Journal of the American Dental Association.* 2003;134(4):434–41.
31. Tamse A, Fuss Z, Lustig J, Kaplavi J. An evaluation of endodontically treated vertically fractured teeth. *J Endod.* 1999;25(7):506–8.
32. Jeffrey P. Okeson D. Management of temporomandibular disorders and occlusion. 8th ed. MOSBY; 2019. 56 p.
33. Gibbs CH, Mahan PE, Lundeen HC, Brehnan K, Walsh EK, Holbrook WB. Occlusal forces during chewing and swallowing as measured by sound transmission. *J Prosthet Dent.* 1981;46(4):443–9.
34. Gibbs CH, Mahan PE, Lundeen HC, Brehnan K, Walsh EK, Sinkewiz SL, et al. Occlusal forces during chewing—Influences of biting strength and food consistency. *J Prosthet Dent.* 1981;46(5):561–7.
35. Silva EJNL, Lima CO de, Barbosa AFA, Lopes RT, Sassone LM, Versiani MA. The Impact of TruNatomy and ProTaper Gold Instruments on the Preservation of the Periradicular Dentin and on the Enlargement of the Apical Canal of Mandibular Molars. *J Endod.* 2022;48(5):650–8.
36. Vorster M, Vyver PJ van der, Markou G, Gravett DZ. The effect of different endodontic access cavity designs in combination with WaveOne Gold and TruNatomy on the fracture resistance of mandibular first molars: A nonlinear finite element analysis. *J Endod.* 2023;0(0).